Human Molecular Genetics, 2017, Vol. 26, No. 18 3545–3552

doi: 10.1093/hmg/ddx239
Advance Access Publication Date: 26 June 2017
Original Article

ORIGINAL ARTICLE

Homozygous *EEF1A2* mutation causes dilated cardiomyopathy, failure to thrive, global developmental delay, epilepsy and early death

Siqi Cao[1,2,3,†], Laura L. Smith[2,†], Sergio R. Padilla-Lopez[4], Brandon S. Guida[4], Elizabeth Blume[5], Jiahai Shi[6], Sarah U. Morton[1], Catherine A. Brownstein[2,3], Alan H. Beggs[2,3], Michael C. Kruer[4] and Pankaj B. Agrawal[1,2,3,*]

[1]Division of Newborn Medicine, [2]Division of Genetics and Genomics, [3]The Manton Center for Orphan Disease Research, [5]Department of Cardiology, Boston Children's Hospital and Harvard Medical School, Boston, MA 02115, USA, [4]Department of Child Health, Barrow Neurological Institute, Phoenix Children's Hospital, University of Arizona College of Medicine, Phoenix, AZ 85013, USA and [6]Department of Biomedical Sciences, City University of Hong Kong, Hong Kong SAR

*To whom correspondence should be addressed at: Divisions of Newborn Medicine and Genetics & Genomics, Boston Children's Hospital, 300 Longwood Ave CLSB 15030, Boston, MA 02115, USA. Tel: +617 9192153; Fax: +617 7300253; Email: pagrawal@enders.tch.harvard.edu

Abstract

Eukaryotic elongation factor 1A (EEF1A), is encoded by two distinct isoforms, *EEF1A1* and *EEF1A2*; whereas *EEF1A1* is expressed almost ubiquitously, *EEF1A2* expression is limited such that it is only detectable in skeletal muscle, heart, brain and spinal cord. Currently, the role of EEF1A2 in normal cardiac development and function is unclear. There have been several reports linking *de novo* dominant *EEF1A2* mutations to neurological issues in humans. We report a pair of siblings carrying a homozygous missense mutation p.P333L in *EEF1A2* who exhibited global developmental delay, failure to thrive, dilated cardiomyopathy and epilepsy, ultimately leading to death in early childhood. A third sibling also died of a similar presentation, but DNA was unavailable to confirm the mutation. Functional genomic analysis was performed in *S. cerevisiae* and zebrafish. In *S. cerevisiae*, there was no evidence for a dominant-negative effect. Previously identified putative *de novo* mutations failed to complement yeast strains lacking the *EEF1A* ortholog showing a major growth defect. In contrast, the introduction of the mutation seen in our family led to a milder growth defect. To evaluate its function in zebrafish, we knocked down *eef1a2* expression using translation blocking and splice-site interfering morpholinos. EEF1A2-deficient zebrafish had skeletal muscle weakness, cardiac failure and small heads. Human *EEF1A2* wild-type mRNA successfully rescued the morphant phenotype, but mutant RNA did not. Overall, EEF1A2 appears to be critical for normal heart function in humans, and its deficiency results in clinical abnormalities in neurologic function as well as in skeletal and cardiac muscle defects.

Introduction

Eukaryotic translation elongation factor 1 alpha (EEF1A) is required for the enzymatic delivery of aminoacyl transfer RNAs (aa-tRNA) to the ribosome during protein biosynthesis. EEF1A is one of four subunits of the EF-1 complex that facilitates the GTP-dependent recruitment of aa-tRNA to the acceptor site of

[†]The authors wish it to be known that, in their opinion, the first 2 authors should be regarded as joint First Authors.
Received: April 20, 2017. **Revised:** June 9, 2017. **Accepted:** June 20, 2017

the ribosomal complex during polypeptide chain assembly. Human EEF1A is found in two isoforms, EEF1A1 and EEF1A2, that are encoded by distinct genes (1). The two proteins share 93% amino acid sequence identity, and either protein isoform is sufficient for translation. However, the promoter sequences upstream of the two genes differ significantly, and their expression patterns are spatiotemporally unique. The EEF1A1 isoform is highly expressed in all tissues during development in humans, but postnatally its expression declines in terminally differentiated cells of the skeletal muscle, heart, and neurons in the brain and spinal cord (2). EEF1A2 is highly expressed in neurons and in those tissues where EEF1A1 expression decreases postnatally. Despite significant sequence homology, the two isoforms are also post-translationally modified at different sites, suggestive of performing distinct functions in addition to their canonical roles (3).

A neurodegenerative "wasted" (*wst*) phenotype has been observed in *Eef1a2*-null mice. The autosomal recessive mutation *wst* arose spontaneously in an inbred colony at the Jackson Laboratory (4) and was found to represent a deletion that encompassed the promoter and first exon of *Eef1a2*, abolishing its expression (5). Homozygous *wst/wst* mice exhibit neurologic defects, muscle wasting, and immune abnormalities.

There is also evidence linking *de novo* dominant *EEF1A2* mutations to neurological deficits, including severe intellectual disability (ID), autistic behavior, absent speech, hypotonia, and epilepsy (6–11). Mutations identified in each case involved missense changes in critical residues that were highly conserved, although functional studies were not performed. In this study, we report the first homozygous *EEF1A2* sequence variant in a family with dilated cardiomyopathy (DCM), global developmental delay (GDD), failure to thrive (FTT), epilepsy and death in early childhood.

Results

Clinical phenotype

The proband (II:1), a male child, was born healthy to a family with a distant history of consanguinity. The proband's family history was significant for early childhood death of two siblings with cardiomyopathy and seizures (pedigree shown in Fig. 1A). The proband's oldest sister (II:3), died at 3 years of age with a diagnosis of DCM. She was also reported to have torticollis, progressive GDD with loss of motor milestones, and seizures. His middle sister (II:2) also had DCM, hepatomegaly, GDD, FTT (Fig. 1C), and a seizure disorder. It was also noted that she was hypertonic, microcephalic and had facial dysmorphism including coarse features, a triangular face, upwards slanted eyes, and a bow shaped mouth with downturned corners. At 5 years of age, she had lost major milestones, was unable to sit unsupported and had a vocabulary of 20 words. Brain MRI at both 1.5 and 4.5 years were normal. Extensive metabolic evaluation was negative. Echocardiography at that time demonstrated severe left ventricular (LV) dysfunction with ejection fraction (EF) of 0.21 (z-score −8.3) and LV mass of 42 grams (95%ile for age), which rapidly progressed. She was deemed not to be a candidate for cardiac transplant, was discharged on palliative inotropes, and died soon after. Neither maternal nor paternal medical histories were significant for encephalopathy, ID or other neurodevelopmental abnormalities; however, the father was unable to make eye contact and would smile inappropriately during medical encounters. Each of the father's three children with a different mother exhibited speech delays. Further, two paternal nieces have learning disability with specific problems in speech/language. In addition, two paternal first cousins and the mother's first cousin have a seizure disorder.

Given his family history, the proband was monitored extensively throughout life. On initial assessment, the proband's heart was structurally and functionally normal. At 3 months, electrocardiogram (EKG) and echocardiogram results showed normal electrical activity and cardiac function. Due to three events concerning for seizure activity, each lasting less than 5 min, further testing was conducted at 8 months of life; at that time both EEG and brain MRI were normal. The proband later suffered two febrile seizures between 10 months and 13 months of life, but his neurological and cardiac exams remained normal.

At 6 months, the proband was first observed to have developmental delays, and at 9 months, had missed age-appropriate gross motor milestones. He, like his older sister, was also noted to have facial dysmorphism, including coarse features, upward slanted eyes, depressed mid face, prominent cheeks, nose with inverted nares, broad nasal bridge, and a thin upper lip. By 18 months, he was unable to pull to a stand, walk, or speak and could only occasionally sit without support. At this time, the proband's cardiac condition began to deteriorate. An echocardiogram revealed a decrease in left ventricular ejection fraction (LVEF) from 0.68 to 0.58. Within the following 3 months, the proband's heart condition worsened with LVEF falling to 0.45 at which time treatment was initiated with diuretics and angiotensin-converting enzyme inhibitor enalapril. There was no evidence of structural abnormalities. The proband's status steadily declined, and by 23 months, he had dilated left ventricle (end diastolic volume of 57.5 ml) (z-score 4.7) with moderate to severe dysfunction (LVEF of 0.31) (z-score −6.2) Between 23 and 26 months, the proband clearly showed signs of FTT: his weight rapidly dropped from 11.4 (19%ile for age) to 10.3 kg (1.4%ile for age) (Fig. 1B) as he regressed from milestones he had previously achieved. It was also noted that the proband had tight heel cords with hypertonia, particularly in the lower extremities. The proband's heart failure and seizure disorder progressed and he continued to lose milestones until he died of heart failure at 29 months.

Mutation analysis

Whole exome sequencing (WES) was performed on genomic DNA from the proband, affected sister, and both parents. The eldest sister was deceased at the time of the study and her DNA was not available. The WES data were evaluated for recessive variants in genes linked to seizures and/or cardiomyopathy. Homozygous missense variants were identified in two genes (Table 1), only one of which has been linked to human disease. A single homozygous missense variant in *EEF1A2* was identified in both affected siblings (hg19: Chr 20: 62121863, c.998C > T leading to p.P333L variant) while the parents were heterozygous (Fig. 1D). The residue P333 is highly conserved across both EEF1A1 and EEF1A2 proteins (Fig. 1E), and the variant p.P333L was deemed pathogenic by several *in silico* software programs, including Polyphen-2, SIFT, and MutationTaster. The exact variant was not present in the gnomAD database (gnomad.broadinstitute.org; date last accessed June 7, 2017) while a different substitution of p.P333S was seen once (1/243694) in heterozygous state.

Molecular modeling of *EEF1A2*

To initiate delivery of aa-tRNA to the A site of the ribosome, EEF1A first forms a ternary complex with aa-tRNA and GTP

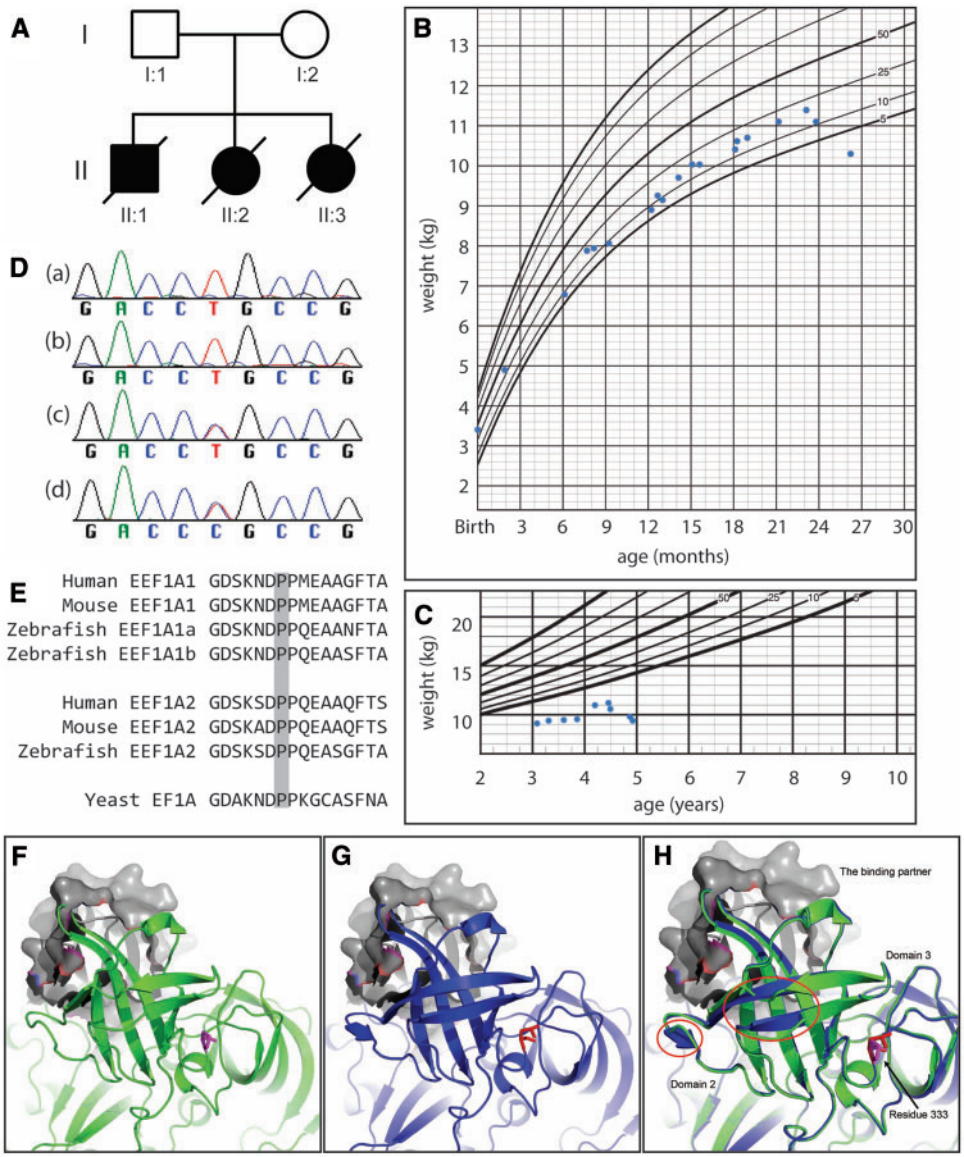

Figure 1. Genetic findings in a family affected by a *EEF1A2* mutation. (**A**) Pedigree of the family carrying the *EEF1A2* mutation. (**B**, **C**) Weight records for proband (II:1)(B) and affected sibling (II:2)(C). (**D**) Sanger sequencing chromatograms for the proband (a), affected sibling (b), mother (c) and father (d). (**E**) Conservation of proline residue at amino acid 333 of EEF1A2 across various species. (**F–H**) Molecular modeling showing the conformational change induced in EEF1A2 by a p.P333L substitution. P333 and L333 are shown in stick with purple and red colors, respectively. The wild-type is colored in green, and the mutant is colored in blue. The potential binding partner is colored in grey.

Table 1. Homozygous recessive variants identified in two affected members of the family

Genes	Genome Assembly	Chromosome	Location	Transcript	cDNA change	aa change	Polyphen-2	SIFT	Mutation Taster	gnomAD (Frequency)
EEF1A2	GRCh37/hg19	20	62121863	NM_001958	cDNA.1164C>T	P333L	probably damaging	deleterious	disease causing	0
SLC2A4RG	GRCh37/hg19	20	62373525	NM_020062	cDNA.674G>A	G208R	probably damaging	deleterious	polymorphism	9/256774 (0.004%)

(aa-tRNA:EEF1A2:GTP). Upon delivery, the ribosome then catalyzes the hydrolysis of GTP to form the inactive EEF1A:GDP, which leaves the A site. Lastly, the inactive form of EEF1A is recycled to the active GTP form via the catalytic activity of EEF1B. EEF1B binds to EEF1A at the same site as the aa-tRNA. Both isoforms of EEF1A contain three structural domains, two of which sandwich EEF1B during binding (domain 1 and 2) (12). A structural model of human EEF1A2 was built based on the structure of yeast

EEF1A (PDB: 1F60) by Modeller (13). The model indicates residue 333 is located at the loop linking domain 2 and 3 at the back of the shared aa-tRNA and EEF1B binding site. Another model with proline to leucine substitution was also built following the same protocol. Interestingly, the mutant has a more stable domain 2 with more defined β-sheets compared to the wild-type (Fig. 1F–H). The change in the dynamic of domain 2 likely changes the binding affinity of EEF1A2 to its binding partners.

TEF1/2 mutation in yeast

Haploid yeast contains two EEF1A orthologs, *tef1* and *tef2*, with ~80% homology to the human gene. We initially performed complementation studies in a *tef2*Δ background with rapamycin challenge media to evaluate the effects of the previously reported (p.G70S) variant (described in association with epileptic encephalopathy) and the (p.P333L) variant we identified. We introduced the P→L substitution in the corresponding site in *tef2* (residue 331) (Fig. 2A). Although (p.G70S) showed a severe growth defect phenotype, no difference was appreciable between (p.P331L) and wild-type (Fig. 2B).

Plasmid shuffling experiments were next performed to mimic and analyze the effect of human *EEF1A2* missense mutations in yeast. Plasmid shuffling is necessary because double knockout of the *tef1* and *tef2* yeast genes is lethal. To circumvent this limitation, the *tef1*- Δ*tef2*-Δ strain is maintained alive by introducing a plasmid expressing *tef1* and the selectable marker *trp1*, which allows tryptophan synthesis. In the plasmid shuffling experiments, the *tef1*- Δ*tef2*-Δ strain was also transformed with the plasmid p416GPD (*ura3* marker) expressing *tef2*-V5 (tef2 with the V5 C-terminal tag) and *tef2*-V5 variants mimicking two *EEF1A2* mutations, (p.G70S) and (p.P331L). In a medium with fluoroanthranilic acid (FAA), yeast cells that are able to synthesize tryptophan convert FAA into the cytotoxic compound 5-methyltryptophan. Therefore, FAA medium selects for colonies that have lost the original *trp1*-*tef2* plasmid, and only have p416GPD-derived plasmids. This experiment tested whether *tef2*-V5 and its variants were able to rescue the lethality of the *tef1tef2*Δ strain when expressed alone, and served as a readout of the functionality of the different variants. Figure 2C shows that the missense mutation (p.G70S) leads to the loss of function of *tef2* (*EEF1A2*), while *tef2* comprising the (p.P331L) variant still retains some functionality, but not as much as wild-type.

eef1A2 knockdown results in zebrafish cardiomyopathy

To investigate the *in vivo* effects of EEF1A2 deficiency in zebrafish development, single-cell embryos were injected with morpholino antisense oligomers (MO) to disrupt *eef1a2* expression. Two different MO were designed to achieve functional gene knockdown, either by blocking translation of zebrafish *eef1a2* mRNA transcripts or by interfering with pre-mRNA splicing at the exon2-intron2 splice site. Standard and quantitative RT-PCR assays and Western blot were used to confirm the efficacy of the *eef1a2* functional knockdown. At 2-day post-fertilization (2dpf), RT-PCR assay detected lower expression and aberrant splicing of *eef1a2* mRNA in zebrafish injected with the splice-site-blocking MO. Further quantification of *eef1a2* and *β-actin* mRNA using qRT-PCR technology confirmed that, compared to WT zebrafish, MO-injected zebrafish embryos exhibited a >8-fold reduction in *eef1a2* mRNA (Fig. 3A). Similarly, Western blot analysis showed that at 2dpf, EEF1A2 protein was nearly absent in zebrafish injected with the translation-blocking MO (Fig. 3B).

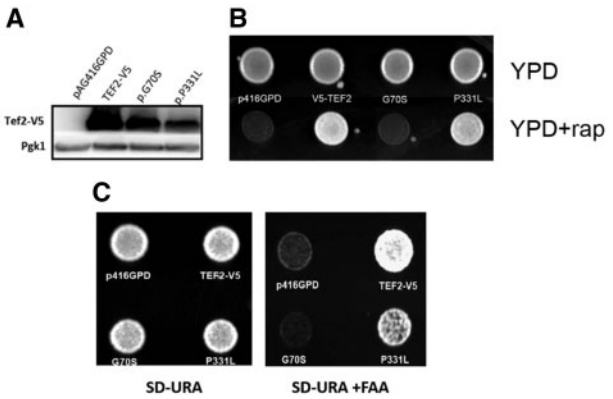

Figure 2. Effect of the expression of *TEF2* variants mimicking human *EEF1A2* mutations in *Saccharomyces cerevisiae*. (**A**) Western blot showing cellular levels of TEF2-V5 and its variants expressed under the GPD promoter in p416GPD plasmid. (**B**) tef2 single mutant show a rapamycin sensitivity phenotype that is complemented by the expression of V5-TEF2 or P331L variant, but not G70S variant. (**C**) In the plasmid shuffling experiments shown above, tef1tef2 strain is transformed with both *pTEF2 TRP1* and p416GPD *URA3* expressing either TEF2-V5 or its variants G70S and P331L. Plating on FAA medium select for the colonies that have lost *pTEF2 TRP1* and only have p416GPD derived plasmids. The figure shows that missense mutation p.G70S lead to the loss of function of Tef2 (EEF1A2) while p.P331L variant still remains some functionality.

Phenotypically, zebrafish injected with either MO appeared similar at 2dpf. At relatively low doses of MO (5 ng), zebrafish had mild to strong dorsal axis curvature and smaller heads, obvious developmental abnormalities (Fig. 3C). As the injected dose of MO increased, the phenotype of the zebrafish became increasingly severe. Increased curvature along the dorsal axis was most apparent, likely related to late hatching caused by muscle weakness (Fig. 3D). Additionally, a comparative analysis between images of the living *eef1a2* MO-injected zebrafish and the wild-type controls from the same clutch indicated that the EEF1A2-deficient zebrafish also showed signs of severe heart failure. These included pericardial effusion and atrial enlargement (Fig. 3E), in addition to irregular and depressed heart rates (Fig. 3F). The consistency in the achieved phenotype across the two different MO suggests that the observed EEF1A2-deficient phenotype is due to the specific MO knockdown of *eef1a2*, rather than to off-target effects. To further confirm the specificity of the EEF1A2-deficient phenotype, rescue experiments were performed with human wild-type *EEF1A2* mRNA and mRNA with the proline to leucine substitution at residue 333 (p.P333L). Compared with MO-injection only, co-injection of MO and both wild-type *EEF1A2* mRNA and p.P333L *EEF1A2* mRNA led to increased deaths; however, over-expression of wild-type *EEF1A2* mRNA led to the recovery of the wild-type phenotype and to fewer affected zebrafish, whereas over-expression of the mutant p.P333L *EEF1A2* mRNA did not improve outcome compared to MO-injected zebrafish (Fig. 3G).

Discussion

We have identified an autosomal recessive missense mutation in *EEF1A2* in a family affected by progressive DCM, GDD, and epilepsy. The proband and the other two affected siblings were phenotypically normal at birth, but postnatally their conditions deteriorated rapidly leading to early death. Many of the clinical presentations in our patients are strikingly similar to reported clinical findings in *de novo* cases summarized in Table 2. For example, similar to our patients, individuals from nearly all other

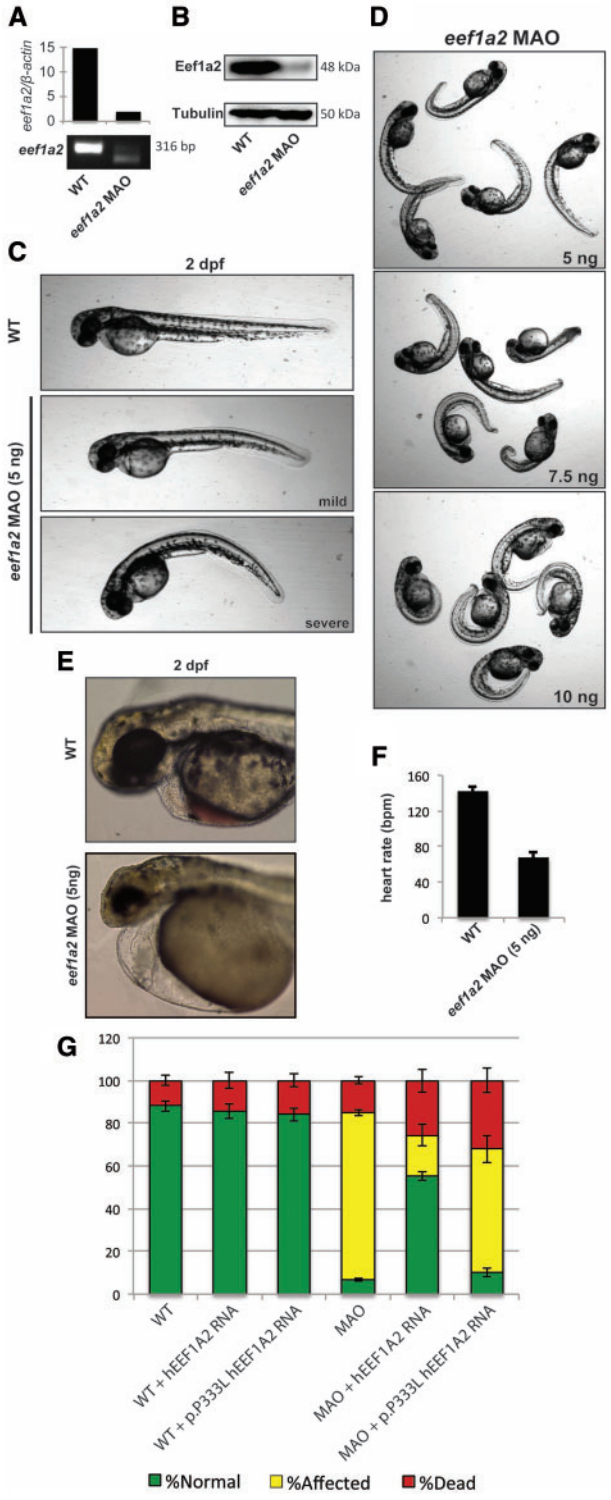

Figure 3. Morpholino-based knockdown of *eef1a2* in developing zebrafish. (**A**) *eef1a2* qRT-PCR and standard RT-PCR demonstrating an 8-fold reduction of mRNA in MO-injected (5 ng) zebrafish embryos. (**B**) Western blot analysis of Eef1a2 protein levels in WT and MO-injected (5 ng) zebrafish embryos using an anti-EEF1A2 antibody. Membranes were restained with tubulin to demonstrate adequate loading of protein in lanes. (**C**) Dorsal curvature in developing zebrafish after injection of 5 ng of MO ranges from mild to severe. (**D**) Dose-dependent response to MO injection at 5 ng, 7.5 ng, and 10 ng. (**E**) Light microscopy of living zebrafish hearts and heads. (**F**) Differences in heart rate between control and MO-injected zebrafish embryos at 2 dpf. (**G**) Rescue experiments in MO-injected zebrafish embryos showing the ability of the WT human *EEF1A2* mRNA to salvage WT phenotype with fewer affected zebrafish while embryos injected with p.P333L human *EEF1A2* mRNA were not rescued and developed a phenotype similar to that of the MO-injected zebrafish.

cases are noted to have facial dysmorphism, seizures, and developmental delay. The only unique finding in our family is DCM suggesting that cardiac function in those with *de novo* mutations needs to be evaluated.

There are also similarities in the phenotype and timing of presentation between our patients and EEF1A2 deficient mice. EEF1A2 is most highly expressed in the brain, spinal cord, skeletal and cardiac muscle of mice, which matches with the phenotype in our patients. EEF1A2 is also most highly expressed postnatally when the expression of EEF1A1 in those tissues begins to decrease (14). Further, *Eef1a2*-null mice exhibit similar symptoms with delay in phenotypic presentation. They were phenotypically normal until weaning, but at approximately 21 days of life, they developed tremors and ataxia, exhibited muscle wasting, and then died in a week (5,15). Given the parallels in symptoms and disease timing between human patients homozygous for the p.P333L mutation and *Ee1f2*-null mice, it seemed likely that the delayed emergence of neurological, developmental, and cardiac symptoms in our patients was due to lower expression of EEF1A1 and the inability of mutant EEF1A2 to compensate in those tissues.

The variant p.P333L has never been seen previously in publicly available databases, including gnomAD, and the affected residue is extremely well conserved. Molecular modelling suggests that residue P333 is located at the loop linking domains 2 and 3, and regulates the dynamics of the loop with proline cis-trans isomerization (16). The variant p.P333L likely changes the dynamics of nearby residues in the loop and the structure of the protein, which may affect the binding affinity of EEF1A2 to its partners such as aa-tRNA and EEF1B.

Our yeast data indicate that the (p.P333L) missense mutation is deleterious given the inability of the mutant to rescue the growth defects seen in *tef1tef2*Δ cells. This finding represents an important functional genomic validation that the homozygous variant is in fact deleterious. Of potential interest, the phenotype seen with the (p.P333L) variant is more subtle than the phenotype occurring with the (p.G70S) mutant strain complementation studies. The fact that a phenotype was readily evident in a tef2D background with the (p.G70S) mutant, while the (p.P333L) mutant required plasmid shuffling studies to demonstrate that it was deleterious, is consistent with the phenotype in human patients. In the human case, heterozygous *de novo* (p.G70S) variants cause encephalopathy, but heterozygous human (p.P333L) carriers do not have such a striking phenotype; only when the (p.P333L) mutation affects both alleles does the lethal phenotype manifest itself. Interestingly, a recent study identified homozygous G70S mutation to be more severe than homozygous *Eef1a2*-null mice needing to be euthanized by P18 compared to P23-28 for the null mice (17).

We have employed zebrafish (*Danio rerio*) as a vertebrate animal model to further elucidate the normal *in vivo* function of EEF1A2 in muscle, heart and brain. Highly conserved throughout eukaryotic evolution, human EEF1A2 shares 94% amino-acid sequence identity with its zebrafish homologue. Additionally, zebrafish are not dependent on a functional cardiovascular system for survival during the early stages of embryo development, making them an excellent vertebrate model

Table 2. Phenotypic presentation of patients with *EEF1A2* mutations

Variant (aa)	Patient	Sex	Developmental Delay	Facial Dysmorphism	MRI	Onset of Epilepsy	Seizures	ID	Cardiac Involvement
P333L	**Case II:1**	M	Global developmental delay	+	normal	7m	absences, tonic-clonic, eye deviation, febrile	+	DCM
P333L	**Case II:2**	F	Global developmental delay	+	normal	12m	febrile, tonic-clonic	+	DCM
G70S	Lam case 1	F	Global developmental delay	+	NR	2m	Myoclonic, tonic-clonic seizures; absences	NR	NR
G70S	deKovel 2008D06721	F	NR	NR	NR	NR	Epileptic encephalopathy	NR	NR
G70S	deLigt Trio91	F	Global developmental delay	–	NR	4m	Myoclonic seizures, grand mal, absences	+	NR
G70S	Veeramah TrioB	M	Non-verbal	NR	NR	infant	Infantile spasms; myoconic, tonic-clonic, seizures	+	NR
E122K	Lam case 5	F	Non-verbal, gross motor delay	+	NR	2m	Infantile spasms	+	NR
E122K	Inui case 2	M	Yes	+	cerebral atrophy	8m	myoclonic seizures, myoclonic–atonic	+	NR
E122K	Inui case 1	F	Yes	+	normal	10m	Myoclonic seizures, atypical absences	+	NR
E122K	Nakajima case 2	F	Motor delay	+	mild atrophy of cerebrum	4m	Infantile spasms	+	NR
R423C	Lam case 7	M	Global developmental delay	+	NR	4m	Multiple daily seizures	+	NR
E124K	Lam case 6	F	Significant delays in language	–	normal	3m	Myoclonic seizures, absences	+	NR
F98L	Lam case 4	F	Global developmental delay	+	NR	infant	Focal, myoclonic, tonic, tonic-clonic seizures	+	NR
D91N	Lam case 3	F	Global developmental delay, nonverbal	+	NR	2yr	Head drops, infantile spasms, atypical absences	+	NR
I71L	Lam case 2	M	Global developmental delay	+	NR	NR	Yes	+	NR
D252H	Nakajima case 1	F	Yes	+	mild atrophy of cerebrum	8yr	Generalized tonic seizures	+	NR

NR = not reported; – = reported as absent.

for the study of a mutation suspected to cause heart failure. In the present study, we are first to show that complete functional knockdown of *eef1a2* in zebrafish gives rise to abnormal development, neurological problems, and heart failure. Additionally, human wild-type *EEF1A2* mRNA successfully rescued this phenotype, while expression of mutant p.P333L *EEF1A2* mRNA was unable to do so. It is important to note, however, that the zebrafish genome contains 4 distinct genes coding for closely related isoforms of EEF1A, and it is likely that injection of MO in excess of target RNA leads to off target effects that are difficult to isolate (18).

In summary, we have identified a homozygous missense mutation in *EEF1A2* associated with a recessive lethal phenotype and multisystem involvement. Further, while heterozygous mutations in *EEF1A2* have been previously linked to early epileptic encephalopathies and intellectual disability, this is the first time that a homozygous mutation in *EEF1A2* has been associated with multisystem involvement including cardiomyopathy, epilepsy, GDD, and early death.

Materials and Methods

Whole exome sequencing

The proband, both parents, and the affected sibling were enrolled in an Institutional Review Board approved study at Boston Children's Hospital (BCH). DNA extraction from blood samples was performed by the Research Connection Biobank Core, and whole exome sequencing (WES) by the Genetics Diagnostics Laboratory at BCH. Total genomic DNA was extracted from peripheral blood lymphocytes using QIAmp DNA Mini Kit (Qiagen). DNA from the enrolled four members of the family was sent for WES. Samples were prepared as an Illumina sequencing library and enriched for exomic sequences using the Agilent V5 Sureselect kit. The captured libraries were sequenced using Illumina HiSeq 2000 Sequencers at Lab Corp. FASTQs generated from exome sequencing were filtered and aligned, and variants were filtered and annotated, as previously described (19).

Complementation in S. *cerevisiae*

Strain MC214 (*MAT α ura3-52 leu2-3,112 trp1-Δ1 lys2-20 met2-1 his4-713 tef1::LEU2 tef2ΔpTEF2 TRP1*) was kindly provided by Dr. Terri Goss Kinzy.

Yeast strains were grown as indicated in YPD medium (1% Yeast extract, 2% peptone, 2% D-glucose) or synthetic complete (SC) medium (6.7 g/l yeast nitrogen base, 2% glucose) supplemented appropriately. For plasmid shuffling experiments, FAA medium containing 5-fluoroanthranilic acid at 0.5 g/l was used as previously described (20).

EEF1A2, V5 N terminal TEF2 cDNA sequences and all their variants analyzed in this work were synthesized using Genscript Inc. and introduced into p416GPD (URA3) vector using BamHI and EcoRI restriction sites, allowing us to express them under the strong promoter GPD. The obtained plasmid was used to transform yeast using the lithium acetate method (21).

Morpholino (MO) knockdown and mRNA rescue

Two MO, one that blocked *eef1a2* translation and one that interfered with pre-*eef1a2* splicing, were designed to knockdown zebrafish *eef1a2*. The sequence of the translation-blocking MO was 5'-GGATCTTCTCTTTCCCCATGTTGAC-3'. The sequence of the splice-site blocking MO was 5'-CATGGAAGATGGACACAT ACCCAGT-3'. MO were dissolved in 1x Danieau buffer (58 mM NaCl, 0.7mM KCl, 0.4 mM $MgSO_4$, 0.6 mM $Ca(NO_3)_2$, 5.0 mM HEPES pH 7.6).

Rescue mRNA was generated using full-length human cDNA for *EEF1A2* (Clone 5741243, Open Biosystems) and standard Gateway Cloning methods. Site-directed mutagenesis (GeneArt) was used to induce a c.998C > T change to create p.P333L mRNA. mRNA was generated *in vitro* using mMessage mMachine (Ambion) and purified with Megaclear (Ambion).

Microinjection of single-cell zebrafish embryos

Single-cell zebrafish embryos were individually microinjected under a dissecting microscope with pulled microcapillary pipettes to deliver MO. The embryos were then incubated in sterile fish water at 37 °C. In rescue experiments, both MO and mRNA solutions were prepared at double concentration and mixed immediately prior to injection.

RNA isolation, reverse transcription and polymerase chain reaction

Total RNA was isolated from pools of 50 zebrafish at 48-h post-fertilization (hpf) using RNeasy Fibrous Tissue Mini Kit (Qiagen). To homogenize zebrafish tissue, 0.5 mm diameter Ceria Stabilized Zirconium Oxide Beads (Next Advance, Inc.) were added and the mixture was agitated for 5 min at maximum speed in a Bullet Blender 24 (Next Advance, Inc.). Total RNA (1 μg) extracted from each pool was reversely transcribed into coding DNA using a SuperScript III First-Strand reverse transcription kit (Qiagen).

RT-qPCR was performed in triplicates using Fast SYBR Green Master Mix (Applied Biosystems) in a 7300 Real Time PCR System (Thermo Fisher Scientific). Endogenous beta-actin was used as a control. Primers for amplification of *eef1a2* and *actb* were: 5'-ACCCAGGACAGATCAGTTCA-3' (*eef1a2*, Forward), 5'-GA TTTGGTCACTCTCCCGCT-3' (*eef1a2*, Reverse), 5'-CGAGCAGGAG ATGGGAACC-3' (*actb*, Forward), 5'-CAACGGAAACGCTCATTGC-3' (*actb*, Reverse).

Western blotting

Total protein was isolated from pools of 30 zebrafish at 48 hpf using 250 μL M-PER Mammalian Protein Extraction Reagent with Complete Mini, EDTA-free protease inhibitor cocktail (Sigma Aldrich). To homogenize zebrafish tissue, 0.5 mm diameter Ceria Stabilized Zirconium Oxide Beads (Next Advance, Inc.) were added, and the mixture was agitated for 5 min at maximum speed in a Bullet Blender 24 (Next Advance, Inc.). Lysate was centrifuged at 13,000 RPM for 10 min at room temperature, and the supernatant was collected and quantified with a BCA Protein Assay Kit (Thermo Fisher).

Approximately 20 μg of protein from each experimental group was mixed with beta-mercaptoethanol and nuPage LDS Sample Buffer (Life Technologies), denatured at 95 °C for 5 min, and loaded onto a nuPage 4 to 12% Bis-Tris Gel (Life Technologies). Proteins were separated on the basis of electrophoretic mobility by applying a DC voltage (80 V, 30 min; 120 V, 120 min) using the XCell SureLock™ system and MOPS SDS Running Buffer (Life Technologies). Separated proteins were transferred to a PVDF membrane by applying a DC voltage (10 V, 20 h; 4 °C) using the XCell SureLock™ system and nuPage Transfer Buffer (Life Technologies).

The membrane was blocked for 1 h with 5% Blotting Grade Non-fat Dry Milk (Bio-Rad) in Tris-buffered saline-T (0.02M TRIZMA® Base, 0.15 M NaCl, 0.1% Tween 20; Sigma-Aldrich) and incubated with rabbit anti-EEF1A2 primary antibody (Abcam; #ab60283) in blocking solution overnight at 4 °C. The membrane was washed for 10 min three times with Tris-buffered saline-T, then incubated with goat anti-rabbit IgG HRP conjugate secondary antibody (Biorad; #170-6515) in blocking solution for 1 h at room temperature. The membrane was washed again with Tris-buffered saline-T, developed for 10 min using SuperSignal® West Pico Chemiluminescent Substrate, and visualized with Bio-Rad ChemiDoc XRS. The membrane was stripped with RestoreTM Western Blot Stripping Buffer (20 min, room temperature) and washed again with Tris-buffered saline-T. This process was repeated with primary antibodies against α/β-Tubulin (Cell Signaling Technology; #2148S). Densitometric analysis was performed using NIH ImageJ software (v1.49; NIH, Bethesda, Maryland, USA), and Eef1a2 protein levels were normalized to those of α/β-Tubulin.

Quantification of zebrafish heart rate

Zebrafish heart rates were quantified at 2 dpf by counting the heartbeats over a period of 60 s. An unpaired two-sample t-test was used to determine statistical significance between Eef1a2-deficient zebrafish to their wild-type clutch mates.

Acknowledgements

This work was performed through the Gene Discovery Core of The Manton Center for Orphan Disease Research at Boston Children's Hospital.

Conflict of Interest statement. None declared.

Funding

National Institute of Health (NIH) grants R01 AR068429 (PBA) and R01 AR044345 (AHB) from NIAMS, U19 HD077671 (PBA and AHB), and R01 HD075802 (AHB) from NICHD, and K08 NS083739 (MCK) from NINDS. Clinician Scientist Development Award

from the Doris Duke Charitable Foundation (MCK), and by the Phoenix Children's Hospital Foundation (MCK). Sanger sequencing was performed by the Molecular Genetics Core Facility of the IDDRC at Boston Children's Hospital, supported by National Institutes of Health grant U54 HD090255 from NICHD.

References

1. Lund, A., Knudsen, S.M., Vissing, H., Clark, B. and Tommerup, N. (1996) Assignment of human elongation factor 1alpha genes: EEF1A maps to chromosome 6q14 and EEF1A2 to 20q13.3. *Genomics*, **36**, 359–361.
2. Knudsen, S.M., Frydenberg, J., Clark, B.F. and Leffers, H. (1993) Tissue-dependent variation in the expression of elongation factor-1 alpha isoforms: isolation and characterisation of a cDNA encoding a novel variant of human elongation-factor 1 alpha. *Eur. J. Biochem.*, **215**, 549–554.
3. Soares, D.C. and Abbott, C.M. (2013) Highly homologous eEF1A1 and eEF1A2 exhibit differential post-translational modification with significant enrichment around localised sites of sequence variation. *Biol. Direct.*, **8**, 29.
4. Shultz, L.D., Sweet, H.O., Davisson, M.T. and Coman, D.R. (1982) 'Wasted', a new mutant of the mouse with abnormalities characteristic to ataxia telangiectasia. *Nature*, **297**, 402–404.
5. Chambers, D.M., Peters, J. and Abbott, C.M. (1998) The lethal mutation of the mouse wasted (wst) is a deletion that abolishes expression of a tissue-specific isoform of translation elongation factor 1alpha, encoded by the Eef1a2 gene. *Proc. Natl Acad. Sci. U S A*, **95**, 4463–4468.
6. de Ligt, J., Willemsen, M.H., van Bon, B.W., Kleefstra, T., Yntema, H.G., Kroes, T., Vulto-van Silfhout, A.T., Koolen, D.A., de Vries, P., Gilissen, C. *et al.* (2012) Diagnostic exome sequencing in persons with severe intellectual disability. *N. Engl J. Med.*, **367**, 1921–1929.
7. Nakajima, J., Okamoto, N., Tohyama, J., Kato, M., Arai, H., Funahashi, O., Tsurusaki, Y., Nakashima, M., Kawashima, H., Saitsu, H. *et al.* (2015) De novo EEF1A2 mutations in patients with characteristic facial features, intellectual disability, autistic behaviors and epilepsy. *Clin. Genet.*, **87**, 356–361.
8. Veeramah, K.R., Johnstone, L., Karafet, T.M., Wolf, D., Sprissler, R., Salogiannis, J., Barth-Maron, A., Greenberg, M.E., Stuhlmann, T., Weinert, S. *et al.* (2013) Exome sequencing reveals new causal mutations in children with epileptic encephalopathies. *Epilepsia*, **54**, 1270–1281.
9. de Kovel, C.G., Brilstra, E.H., van Kempen, M.J., Van't Slot, R., Nijman, I.J., Afawi, Z., De Jonghe, P., Djemie, T., Guerrini, R., Hardies, K. *et al.* (2016) Targeted sequencing of 351 candidate genes for epileptic encephalopathy in a large cohort of patients. *Mol. Genet. Genomic Med.*, **4**, 568–580.
10. Inui, T., Kobayashi, S., Ashikari, Y., Sato, R., Endo, W., Uematsu, M., Oba, H., Saitsu, H., Matsumoto, N., Kure, S. *et al.* (2016) Two cases of early-onset myoclonic seizures with continuous parietal delta activity caused by EEF1A2 mutations. *Brain Dev.*, **38**, 520–524.
11. Lam, W.W., Millichap, J.J., Soares, D.C., Chin, R., McLellan, A., FitzPatrick, D.R., Elmslie, F., Lees, M.M., Schaefer, G.B., study, D.D.D. *et al.* (2016) Novel de novo EEF1A2 missense mutations causing epilepsy and intellectual disability. *Mol. Genet. Genomic Med.*, **4**, 465–474.
12. Andersen, G.R., Pedersen, L., Valente, L., Chatterjee, I., Kinzy, T.G., Kjeldgaard, M. and Nyborg, J. (2000) Structural basis for nucleotide exchange and competition with tRNA in the yeast elongation factor complex eEF1A:eEF1Balpha. *Mol. Cell*, **6**, 1261–1266.
13. Webb, B. and Sali, A. (2014) Comparative Protein Structure Modeling Using MODELLER. *Curr. Protoc. Bioinformatics*, **47**, 5 6 1–32.
14. Khalyfa, A., Bourbeau, D., Chen, E., Petroulakis, E., Pan, J., Xu, S. and Wang, E. (2001) Characterization of elongation factor-1A (eEF1A-1) and eEF1A-2/S1 protein expression in normal and wasted mice. *J. Biol. Chem.*, **276**, 22915–22922.
15. Newbery, H.J., Loh, D.H., O'Donoghue, J.E., Tomlinson, V.A., Chau, Y.Y., Boyd, J.A., Bergmann, J.H., Brownstein, D. and Abbott, C.M. (2007) Translation elongation factor eEF1A2 is essential for post-weaning survival in mice. *J. Biol. Chem.*, **282**, 28951–28959.
16. Krieger, F., Moglich, A. and Kiefhaber, T. (2005) Effect of proline and glycine residues on dynamics and barriers of loop formation in polypeptide chains. *J. Am. Chem. Soc.*, **127**, 3346–3352.
17. Davies, F.C., Hope, J.E., McLachlan, F., Nunez, F., Doig, J., Bengani, H., Smith, C. and Abbott, C.M. (2017) Biallelic mutations in the gene encoding eEF1A2 cause seizures and sudden death in F0 mice. *Sci. Rep.*, **7**, 46019.
18. Schulte-Merker, S. and Stainier, D.Y. (2014) Out with the old, in with the new: reassessing morpholino knockdowns in light of genome editing technology. *Development*, **141**, 3103–3104.
19. Thaker, V.V., Esteves, K.M., Towne, M.C., Brownstein, C.A., James, P.M., Crowley, L., Hirschhorn, J.N., Elsea, S.H., Beggs, A.H., Picker, J. *et al.* (2015) Whole exome sequencing identifies RAI1 mutation in a morbidly obese child diagnosed with ROHHAD syndrome. *J. Clin. Endocrinol. Metab.*, **100**, 1723–1730.
20. Toyn, J.H., Gunyuzlu, P.L., White, W.H., Thompson, L.A. and Hollis, G.F. (2000) A counterselection for the tryptophan pathway in yeast: 5-fluoroanthranilic acid resistance. *Yeast*, **16**, 553–560.
21. Ito, H., Fukuda, Y., Murata, K. and Kimura, A. (1983) Transformation of intact yeast cells treated with alkali cations. *J. Bacteriol.*, **153**, 163–168.